ecosystems: how C–N interactions restrict responses to CO_2 and temperature. *Wat. Air Soil Pollut.* **64,** 327–344 (1992).
19. Tietema, A., Emmett, B. A., Gundersen, P., Kjønaas, O. J. & Koopmans, C. The fate of ^{15}N-labelled nitrogen deposition in coniferous forest ecosystems. *Forest Ecol. Mgmt* **101,** 19–27 (1998).
20. Schleppi, P. *et al.* Simulation of increased nitrogen deposition to a montane forest ecosystem: partitioning of the added ^{15}N. *Wat. Air Soil Pollut.* (in the press).
21. Nadelhoffer, K. J. *et al.* The fate of ^{15}N-labelled nitrate additions to a northern hardwood forest in eastern Maine, USA. *Oceologia* **103,** 292–301 (1995).
22. Nadelhoffer, K. J., Downs, M. R., Fry, B., Magill, A. & Aber, J. D. Controls on N retention and exports in a fertilized watershed. *Environ. Monitor. Assess.* (in the press).
23. Nadelhoffer, K. J., Downs, M. R. & Fry, B. Sinks for N additions to an oak forest and a red pine plantation at the Harvard Forest, Massachusetts, USA. *Ecol. Appl.* **9,** 72–86 (1999).
24. Emmett, B. A. *et al.* Predicting the effects of atmospheric nitrogen deposition on conifer stands: evidence from the NITREX ecosystem-scale experiments. *Ecosystems* **1,** 352–360 (1998).
25. Magill, A. H., Downs, M. R., Nadelhoffer, K. J., Hallett, R. A. & Aber, J. D. Forest ecosystem response to four years of chronic nitrate and sulfate additions at Bear Brooks Watershed, Maine, USA. *Forest Ecol. Mgmt* **84,** 29–37 (1996).
26. Magill, A. H. *et al.* Biogeochemical response of forest ecosystems to simulated chronic nitrogen deposition. *Ecol. Appl.* **7,** 402–415 (1997).
27. McNulty, S. G., Aber, J. D. & Boone, R. D. Spatial changes in forest floor and foliar chemistry of spruce-fir forests across central New England. *Biogeochemistry* **14,** 13–29 (1991).
28. Gundersen, P., Callesen, I. & de Vries, W. Nitrate leaching in forest ecosystems is related to forest floor C/N ratios. *Environ. Pollut.* **102,** 403–407 (1998).
29. Abrahamsen, G., Stuanes, A. & Tveite, B. *Long-Term Experiments with Acid Rain in Norwegian Forest Ecosystems. Ecological Studies* Vol. 104 (Springer, New York, 1993).
30. Hauck, R. D., Meisinger, J. J. & Mulvaney, R. L. in *Methods of Soil Analysis, Part 2: Microbiological and Chemical Properties* (eds Weaver, R. W., Angle, J. S. & Bottomly, J. S.) (Soil Science Society of America, Madison, WI, 1994).

Acknowledgements. This research was funded in part by the Commission of European Communities NITREX Project, the US National Science Foundation and the US–Norway Fulbright Program.

Correspondence and requests for materials should be addressed to K.J.N. (e-mail: knute@mbl.edu).

The *mahogany* protein is a receptor involved in suppression of obesity

Deborah L. Nagle*, Sonja H. McGrail*, James Vitale*, Elizabeth A. Woolf*, Barry J. Dussault Jr*, Lisa DiRocco*, Lisa Holmgren*, Jill Montagno*, Peer Bork†‡, Dennis Huszar*, Victoria Fairchild-Huntress*, Pei Ge*, John Keilty*, Chris Ebeling§, Linda Baldini§, Julie Gilchrist§, Paul Burn‖, George A. Carlson§ & Karen J. Moore*

** Millennium Pharmaceuticals, Inc., 640 Memorial Drive, Cambridge, Massachusetts 02139, USA*
† European Molecular Biology Laboratories, Meyerhöfstrasse 1, 69012 Heidelberg, Germany
‡ Max-Delbrück-Centrum für Molekulare Medizin, Robert-Rössle-Strasse 10, 13092 Berlin Germany
§ McLaughlin Research Institute for Biomedical Sciences, 1520 23rd Street South, Great Falls, Montana 59405, USA
‖ Hoffman-La Roche, Inc., Department of Metabolic Diseases, Nutley, New Jersey 07110, USA

Genetic studies have shown that mutations within the *mahogany* locus[1] suppress the pleiotropic phenotypes, including obesity, of the *agouti-lethal-yellow* mutant[2,3]. Here we identify the *mahogany* gene and its product; this study, to our knowledge, represents the first positional cloning of a suppressor gene in the mouse. Expression of the *mahogany* gene is broad; however, *in situ* hybridization analysis emphasizes the importance of its expression in the ventromedial hypothalamic nucleus, a region that is intimately involved in the regulation of body weight and feeding. We present new genetic studies that indicate that the *mahogany* locus does not suppress the obese phenotype of the melanocortin-4-receptor null allele[4] or those of the monogenic obese models (*Lep^{db}*, *tub* and *Cpe^{fat}*). However, *mahogany* can suppress diet-induced obesity, the mechanism of which is likely to have implications for therapeutic intervention in common human obesity. The amino-acid sequence of the *mahogany* protein suggests that it is a large, single-transmembrane-domain receptor-like molecule, with a short cytoplasmic tail containing a site that is conserved between *Caenorhabditis elegans* and mammals. We propose two potential, alternative modes of action for mahogany: one draws parallels with the mechanism of action of low-affinity proteoglycan receptors such as fibroblast growth factor and transforming growth factor-β, and the other suggests that mahogany itself is a signalling receptor.

Signalling from α-melanocyte-stimulating factor (α-MSH) through the melanocortin receptors Mc1r and Mc4r regulates pigmentation and body weight, respectively. Overexpression of agouti, an antagonist of Mc1r and Mc4r (refs 5, 6), results in yellow, obese mice. The murine *mahogany* gene (*mg*) acts in a dosage-dependent manner within the agouti pathway to compensate for agouti overexpression and for lack of signalling from an *Mc1r* null allele[2,3,7]. Mice homozygous for both *mg* and a null allele of *Mc1r* (recessive yellow, *Mc1^{e}*) are yellow, as are *Mc1r^{e}*/*Mc1r^{e}* mice, indicating that *mg* does not act downstream of *Mc1r* (ref. 2). We performed a similar experiment with obese *Mc4r* (ref. 4) knockout mice (Fig. 1). For both sexes, all the animals homozygous for the *Mc4r* null allele were roughly equally obese and were heavier than wild-type mice, independently of the *mg* genotype. These data strengthen and confirm the data obtained with *Mc1r* knockouts, strongly indicating that *mg* acts at or upstream of both melanocortin receptors.

It has been assumed that *mg* acts specifically within the agouti pathway. We tested this by asking whether *mg* can suppress the obesity of other monogenic obese mouse mutants and whether it can suppress diet-induced obesity. We set up appropriate genetic crosses to produce mice that segregated *mg* and one of the mouse obesity mutations, *Cpe^{fat}*, *tub*, or *Lepr^{db}*. No suppression of obesity by *mg* was seen for any of the monogenic obese mutants (Fig. 2a–c), lending credence to the assumed specificity of action of *mg* within the agouti pathway. To determine whether *mg* can suppress diet-induced obesity, we weaned C3HeB/FeJ-*mg^{3J}* and C3H/HeJ mice onto either normal chow (physiological fuel value (PFV) 3.63 kcal g^{-1} with 9% fat) or a high-fat diet (PFV 4.53 kcal g^{-1} with 42.2% fat). Converting the grams of food consumed to calories indicated that male C3H/HeJ mice fed on normal chow or the high-fat diet consumed ~97 kcal per week and 96 kcal per week, respectively; male C3HeB/FeJ-*mg^{3J}* mice fed on normal chow or the high-fat diet consumed ~83 kcal per week and ~81 kcal per week, respectively. Despite the equal calorie intake, the C3H/HeJ mice on the high-fat diet gained more weight than the C3H/HeJ mice fed on normal chow (P=0.0004). In contrast, the C3HeB/FeJ-*mg^{3J}* mice on either diet showed no statistically significant difference in weight (Fig. 2d). Female data (not shown) showed the same trends, although there

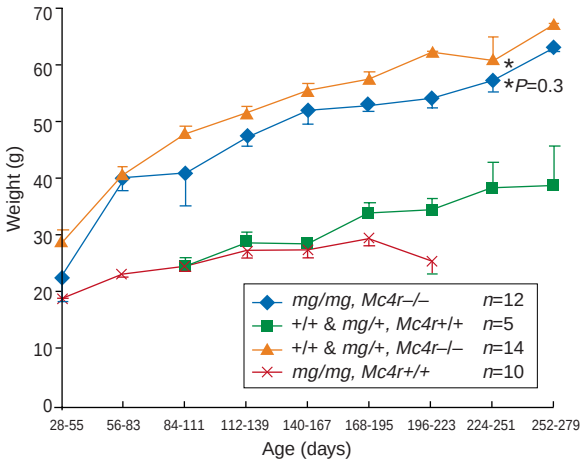

Figure 1 Effect of *mg* on *Mc4r*$^{-/-}$-induced weight gain in females. Values shown are the means ± s.d. within a designated time interval. We performed a *t*-test on the weights of *mg*/*mg*, *Mc4r*$^{-/-}$ animals and +/+, *Mc4r*$^{-/-}$ or *mg*/+, *Mc4r*$^{-/-}$ animals at days 224–251 and found no statistically significant differences in either the female or the male (data not shown) data.

was no statistical significance between any of the mice on either diet.

To identify the *mg* gene we undertook a positional cloning strategy. Multiple genetic crosses produced second-generation mice (n=2437) segregating *mg* that were used to localize the *mg* locus genetically to ~0.6 centimorgans (cM) (Fig. 3b). We created a 1 megabase contig (Fig. 3c) around the *mg* locus containing 30 bacterial artificial chromosomes (BACs), most of which were made into random sheared libraries for shotgun sequencing. At the end of this project we estimated 85% sequence coverage across this ~0.6-cM interval and believe that we have found all genes within the region. We identified 29 genes, 15 of which are novel (Fig. 3d). Within the final minimal interval for *mg*, indicated by a purple line in Fig. 3, there were 11 genes, 9 of which were unknown. We tested all 11 as candidates for *mg* by examining the three mutant alleles of the *mahogany* locus, the original allele, *mg*, that arose in a stock of Swiss × C3H mice, and two alleles that arose independently on the C3H background (C3HeB/FeJ-mg^{3J}/mg^{3J} and C3H/He-mg^{L}/mg^{L}) by northern blot analysis, Southern blot analysis, reverse transcription polymerase chain reaction (RT-PCR) and single-strand conformation polymorphism (SSCP) analysis of genomic PCR products designed to cover the intron–exon boundaries of most of each gene. In all, we analysed 20 genes in this way, one of which showed differences between the wild-type and mutant alleles on a northern blot (Fig. 4a).

The wild-type expression pattern of this gene gives three bands of size ~9 kilobases (kb), 4.5 kb and 3.8 kb, of which the largest is the most prominent (Fig. 4a). The smaller two can be seen in all tissues, but, depending on the tissue, may require extended exposure. Each of the different *mg* alleles gave a different expression pattern. For further clarification of genetic marker order we mapped many of the STSs and ESTs to the Millennium BSB ((C57BL/6J × SPRET/Eij) × C57BL/6J) mapping panel[26] (Fig. 3a). C3HeB/FeJ-mg^{3J}/mg^{3J} has extremely low expression; the 9-kb message only appeared, very faintly, in brain, hypothalamus and fat on northern blots. C3H/He-mg^{L}/mg^{L} expresses a single aberrant band of ~9.5–10 kb in kidney, heart, muscle, fat and, most prominently, in the brain and hypothalamus. LDJ/Le-*mg*/*mg* shows an altered ratio of the three wild-type messages: the 9-kb message is reduced whereas the two smaller messages are more highly expressed, being very abundant in fat and hypothalamus in particular. *In situ* analysis of wild-type brain shows that *mg* is expressed throughout, notably in the hippocampus. Low-power (magnification ×200) examination of *mg* hybridization to wild-type (Fig. 4b, top panel) and LDJ/Le-*mg*/*mg* (data not shown) brains appears equivalent, whereas hybridization to C3HeB/FeJ-mg^{3J}/mg^{3J} brain shows an overall reduction of expression in all regions (data not shown), consistent with the northern blot data. High-power (×400) evaluation of the hypothalamic region revealed an allele-specific reduction of expression in the ventromedial hypothalamic nucleus (VMH) of LDJ/Le-*mg*/*mg* brains (Fig. 4b, LDJ/Le-*mg* VMH image) compared with wild-type brains (Fig. 4b, C3H/HeJ VMH image). Although the VMH is not the only brain region that shows *mahogany* expression, it is the only place in which differential expression in mutant alleles was observed. The altered pattern of expression seen in the VMH of LDJ/Le-*mg*/*mg* mice is particularly interesting, as many neuropeptides and receptors known to be involved in body-weight regulation are expressed there, including *Mc4r* (ref. 8).

We originally identified two overlapping mouse complementary DNAs of 1,051 base pairs (bp) and 2,419 bp. We used these cDNAs as a starting point and, by using both the public expressed sequence

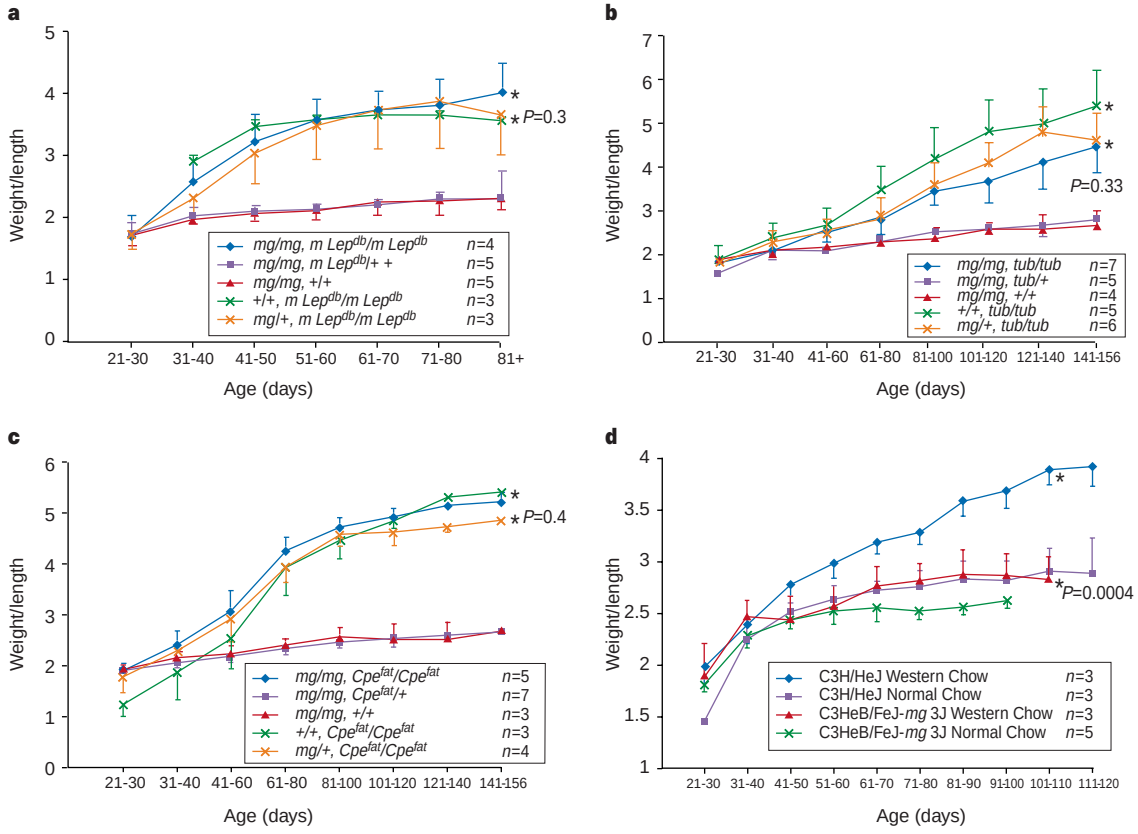

Figure 2 Effect of *mg* on the monogenic obese mutants *tub*, Cpe^{fat} and $Lepr^{db}$ and on obesity induced by a high-fat diet. The values depicted are the means ± s.d. of weight:length ratios. **a–c**, The affect of *mg* on **a**, *tub*, **b**, Cpe^{fat} and **c**, $Lepr^{db}$ mutations in females. We performed *t*-tests on the weight:length ratios of the mice that were genotypically *mg*/*mg*, *mutant*/*mutant* versus +/+, *mutant*/*mutant* (indicated by asterisks). No statistically significant differences were found in either the female or the male (data not shown) data. **d**, Effect of *mg* on diet-induced obesity. Male data are shown. A *t*-test was performed on the weight:length ratios of animals in the C3H/HeJ and C3HeB/FeJ-mg^{3J} classes (indicated by asterisks) fed a western diet at days 101–110 and a statistically significant difference was found, P=0.0004.

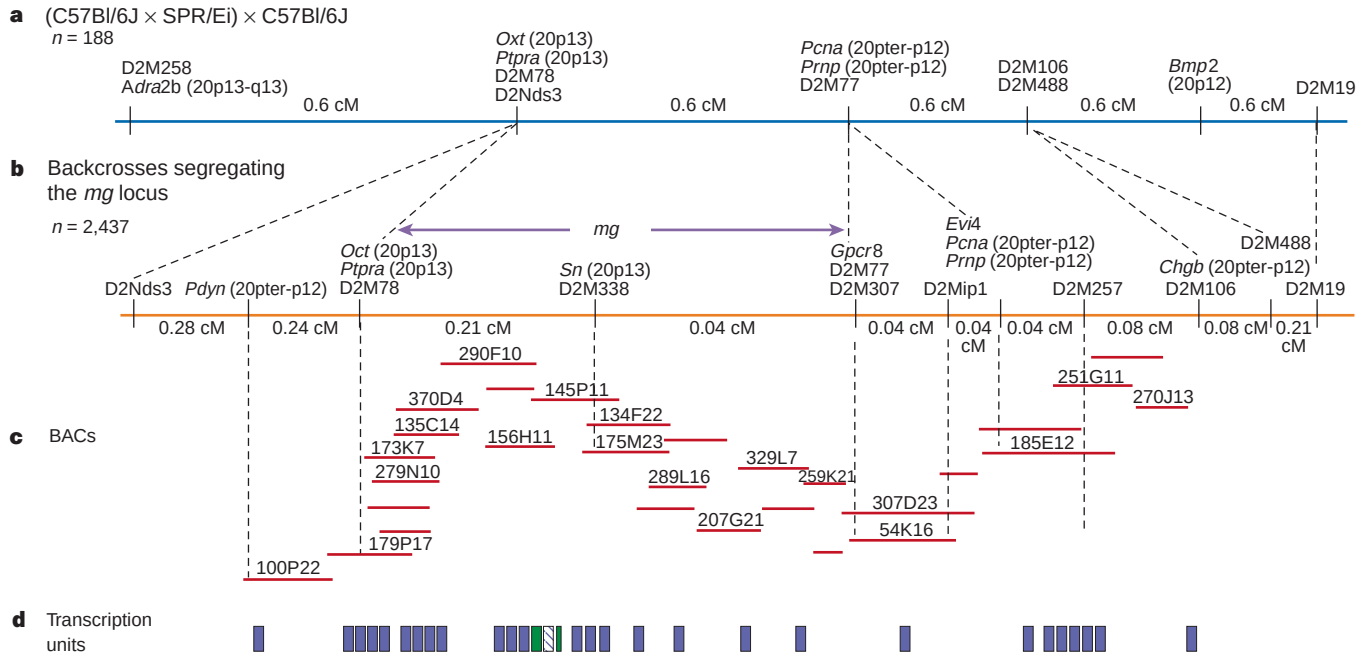

Figure 3 Genetic and physical map of the region surrounding the *mg* locus. All Mit markers are presented with shortened names; for example, *D2Mit77* is shown as *D2M77*. For loci also mapped on the human cytogenetic map, the location is indicated in parentheses after the gene symbol. Genetic distances are given in cM. **a**, The genetic map of the *mg* gene region on the Millennium BSB mapping panel[26]. **b**, The genetic map obtained from crosses segregating *mg* mutant alleles. Relative positions of loci mapped in both the BSB panel and the *mg* segregating crosses are indicated by dashed lines. **c**, The ~1-megabase BAC contig across the *mg* gene region of chromosome 2. BACs used to construct random-sheared libraries for sequencing are labelled with their full name, and are represented by lines that are roughly proportional to their physical size and positioned relative to their physical overlaps. **d**, Transcription units identified here. Each box represents an individual transcription unit. The filled green box identifies the *mg* gene. The hatched box represents a member of the high-mobility-group gene family and sits between coding exons 21 and 22 of the *mg* gene. The map location of the human orthologue of *mg* was determined using both the Genbridge[27] and the G3 (ref. 28) radiation hybrid panels. *mg* maps to human chromosome region 20p13, as predicted, and does not segregate with D20S752.

tag (EST) database and our own, as well as by identifying two cDNA clones from a human liver library, we have been able to build over 7,990 bp of human sequence. The derived human sequence allowed us to estimate the intron–exon boundaries within the mouse genomic sequence; these boundaries were verified by PCR amplification and sequencing. In total we have 6,487 bp of mouse sequence. The mouse genomic locus spans over 160 kb and has 30 identified exons, at least one of which is differentially spliced.

We sequenced the mutant alleles, checking all intron–exon boundaries. A 5-bp deletion at nucleotide 2,809 was found in the coding sequence of the *mg* gene from C3HeB/FeJ-mg^{3J}/mg^{3J}; this deletion introduces a stop codon at codon 937 of the sequence, two codons 3′ of the deletion, resulting in a severely truncated protein lacking many interesting domains (see below). We have not yet identified primary DNA mutations for the other alleles. The combined northern blot analysis, *in situ* hybridization analysis and sequence analysis of the mutant mg^{3J} allele led us to believe that we have identified the mouse *mahogany* gene.

The 4, 011-bp open reading frame (ORF) of mouse *mg* predicts a 1,336-amino-acid polypeptide with a relative molecular mass of 148,706. BLAST searches of the NCBI and SwissProt protein databases identified two human paralogues with a similar modular architecture (KIAA0534, GenBank accession number 3043592, and MEGF8, GenBank accession number AB011541), as well as a *C. elegans* homologue (YC81_CAEEL, GenBank accession number Q19981) (Fig. 5a).

The SMART[9] domain tool revealed sequence motifs in the mahogany polypeptide that provide further clues to its biological function (Fig. 5b). The single-transmembrane-domain mahogany protein has a large extracellular sequence of 1,289 amino acids, which contains three epidermal growth factor (EGF) domains[10], two laminin-like EGF repeats, a CUB domain[11], two plexin-like repeats[12], a C-type lectin[13,14] and seven consecutive Kelch repeats[15] (Fig. 5b) Multiple EGF domains are commonly found in type I membrane proteins (membrane proteins with their amino terminus in the cytosol) that are involved in cell adhesion and receptor–ligand interactions[9]. Laminin-like EGF modules are found in several proteoglycans such as perlecan and heparin sulphate proteoglycan. As CUB domains also occur frequently in glycosylated proteins and as C-type lectins bind carbohydrate, we predict that mahogany is heavily glycosylated and that carbohydrate interactions are essential for the function of mahogany.

Many Kelch-motif-containing proteins have been found that, like mahogany, have multiple consecutive domains. Such consecutive four-stranded β-sheets Kelch motifs form a bladed β-'propeller fold' that is common in many sialidases and other enzymes[14]. Unlike other well-recognized domains, the 'plexin' repeat is less well defined. It was first recognized as a triple repeat in the *Xenopus* protein plexin, which shows similarity to the proto-oncoprotein MET[12]. Since then, this cysteine-rich repeat has been found in six MET gene family members[11], three of which signal through tyrosine kinase and three of which are proposed to have signalling function through a new conserved cytoplasmic domain. The cytoplasmic tail of mahogany is short (126 amino acids) and has no previously defined signalling domain. However, an 8-amino-acid stretch is conserved in proteins (Fig. 5a) from human, mouse and *C. elegans*. The conservation of sequence across such widely evolutionary divergent species strongly indicates that it is a functional domain, possibly a signalling motif.

The multidomain structure of mahogany is complex but shows many similarities to receptor and receptor-like proteins. We predict that mahogany is a large, membrane-spanning protein, with multiple extracellular domains that may have a binding or gathering function as well as a highly conserved putative signalling motif in

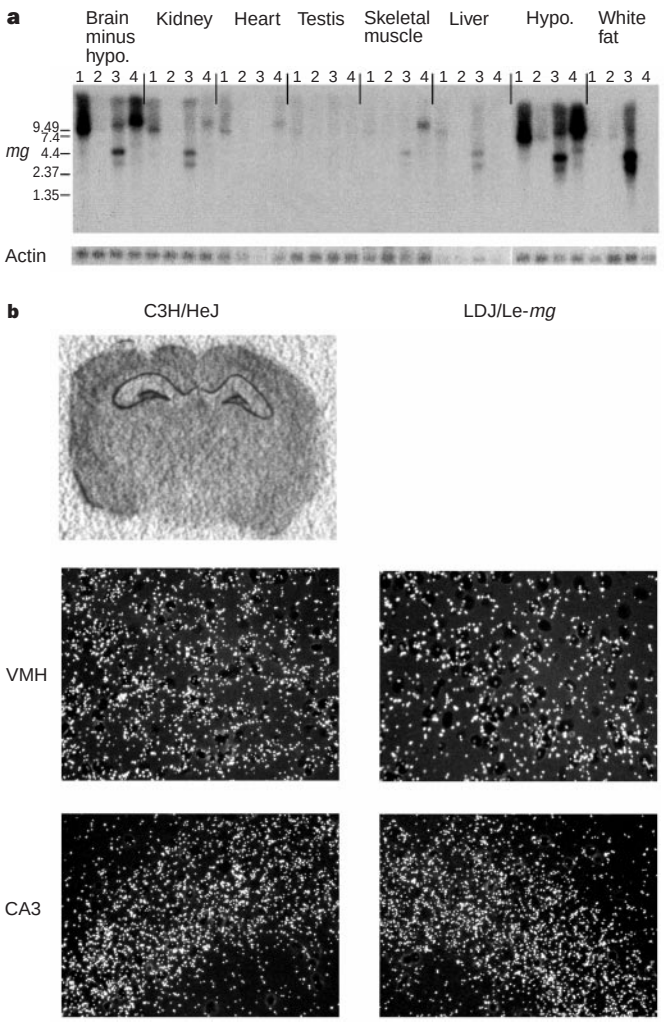

Figure 4 Expression patterns of *mg*. **a**, Northern blot analysis of *mg*, showing expression of C3H/HeJ (lane 1) and the three mutant alleles of *mg*: C3HeB/FeJ-*mg*^{3J} (lane 2), LDJ/Le-*mg* (lane 3) and C3H/HeJ-*mg*^{L} (lane 4). Size markers are on the left. Hybridization with actin is shown below as a loading comparison. **b**, Altered expression of *mg* in the neurons of the VMH. Top panel, an antisense autoradiographic image of a C3H/HeJ brain at the level of the third ventricle, showing that *mg* is expressed widely throughout the mouse brain (original magnifcation ×200). Bottom panels, further evaluation of selected antisense dark-field images show decreased *mg* expression in LDJ/Le-*mg* mutants compared with in C3H/HeJ brain in the region of the VMH but not in the CA3 region of the brain (original magnification ×400).

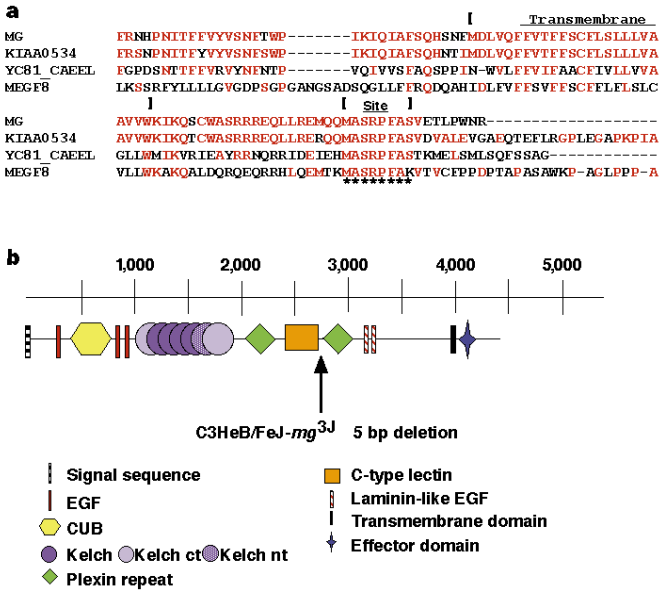

Figure 5 Domains of the mahogany protein. **a**, Alignment of the mahogany protein sequence with its family members (see text), showing the transmembrane domain and cytoplasmic tail. The alignment was performed using CLUSTAL W version 1.5 (ref. 29). Residues highlighted in red indicate conservation between at least two of the four proteins shown. The transmembrane region is indicated within the brackets. The site conserved among all four proteins is indicated by asterisks. KIAA0534 and MEGF8, two human paralogues; YC81_CAELL, a *C. elegans* homologue. **b**, The molecular modular architecture of the mahogany protein. Upon folding of the protein the two Kelch units annotated as ct form the C-terminal (ct) Kelch domain. The Kelch domain annotated as nt is the N-terminal Kelch domain in the folded protein.

the cytoplasmic tail. It is possible that mahogany acts as an accessory receptor, gathering extracellular molecules that are presented to high-affinity receptors, which subsequently signal. Examples of such accessory receptors include the transforming growth factor-β betaglycan receptor, the insulin growth factor-2 receptor and the proteoglycan fibroblast growth factor receptor[16]. It is unclear whether the similarity of mahogany to proteoglycans is meaningful in this regard. Genetic and biological evidence indicates that mahogany probably cannot act to present ligand to the melanocortin receptors, as this would be dichotomous with the antagonism of these receptors by agouti and agouti-related protein[17,18]. Instead, mahogany could present the antagonists to the receptors, thereby reducing signalling. Reduced expression of mahogany would result in increased signalling. An alternative model could simply be that mahogany sequesters away the ligand, effectively increasing the concentration of antagonists in the environment. A similar mechanism of sequestering leptin away from the leptin receptor, thereby reducing signalling and downstream production of proopiomelanocortin products, including α-MSH, is also feasible, yet less likely. The identification of the *mahogany* protein is a major first step towards a better understanding of its role in the agouti pathway, in the reported hyperphagia and hypermetabolic behaviour of *mg* mutants[3] and in suppressing diet-induced obesity, and may open the way to new therapeutic intervention in common human obesity. *Note added in proof*: Since the submission of this manuscript the sequence of the *mg* gene has been published by another group under the name attractin. Attractin is described as a haematopoietic-specific, secreted T-cell activated protein[30]. We have also, since submission of this manuscript, identified alternative splice forms of the *mg* gene, two of which constitute secreted forms. □

Methods

Weight analysis. All animals were multiply housed, but segregated by sex and genotype, and were fed a 9% fat chow diet *ad libitum*, except as noted. Animals were weighed and their lengths were measured every ten days, unless otherwise stated. A weight:length ratio for each animal was generated at each time point.

Mc4r$^{-/-}$ (ref. 7) males and LDJ/Le-*mg*/*mg* females were mated. Resulting F_1 mice were intercrossed, and the F_2 mice were genotyped for the *Mc4r* knockout locus and assayed for coat colour. *mg* heterozygotes could not be distinguished from wild-type mice and were combined into a single group for these analyses. Animals were weighed every 20 days. A Student's *t*-test was performed on the weights of animals that were genotypically *mg*/*mg*, *Mc4r*$^{-/-}$ and on +/+, *Mc4r*$^{-/-}$ or *mg*/+, *Mc4r*$^{-/-}$ animals at days 224–251. To measure the effect of *mg* on monogenic obese mutants, genetic crosses between *tub*, *Cpe*^{fat}, and *Lepr*^{db} animals were performed to produced mice carrying 0, 1 or 2 copies of *mg* with 0, 1 or 2 copies of each of the mutant alleles. The parental strains for these crosses were C57BL/6J-*tub*/*tub* and LDJ/Le-*mg*/*mg*, C57BL/KsJ-*fat*/+ and LDJ/Le-*mg*/*mg*, and C57BL/KsJ-*Lepr*^{db}/+ and LDJ/Le-*mg*/*mg*. We performed *t*-tests on the weight:length ratios of the mice that were genotypically *mg*/*mg*, *mutant*/*mutant* versus +/+, *mutant*/*mutant*.

To assess the affect of *mg* on obesity induced by a high-fat diet, we fed C3H/

HeJ and C3HeB/FeJ-*mg*^{3J} siblings *ad libitum* on either a 9% fat chow diet or a high-fat diet (42.2% fat), formula TD88137 (Harlan Teklad, Madison, Wisconsin). We performed a *t*-test on the weight:length ratios of animals in the C3H/HeJ and C3HeB/FeJ-*mg*^{3J} classes fed a western diet at days 101–110 and found a statistically significant difference, P=0.0004.

Genetic mapping. The crosses and the number of animals for each (n) were (LDJ/Le-*mg*/*mg* × CAST/Ei) × LDJ/Le-*mg*/*mg* (n=1,588), (C3HeB/FeJ-*mg*^{3J}/*mg*^{3J} × CAST/Ei) × C3HeB/FeJ-*mg*^{3J}/*mg*^{3J} (n=324), (C3HeB/FeJ-*mg*^{3J}/*mg*^{3J} × MOLF/Ei) × C3HeB/FeJ-*mg*^{3J}/*mg*^{3J} (n=216) and (C3HeB/FeJ-*mg*^{3J}/*mg*^{3J} × C57BL/6J) × C3HeB/FeJ-*mg*^{3J}/*mg*^{3J} (n=309). The 2,437 F_2 mice were analysed by coat colour to determine their genotype at the *mg* locus. As mice change colour slightly at each hair moult and because the phenotype differences between *mg*/*mg* versus *mg*/+ mice can be subtle, all mice were phenotyped at the same age by a single person. Genomic DNA was analysed for multiple simple sequence length repeat polymorphism (SSLP) markers[19]. With the first ~100 mice we determined that *mg* mapped roughly 15 cM proximal to *agouti* between markers *D2Mit19* and *D2Nds3* (Fig. 3). All remaining animals were genotyped for these markers. Animals recombinant in that interval were typed with all available Mit markers between and for the ever-growing number of markers developed during the project, totalling 265 markers. They are available as a list of PCR primers from the authors.

Sequence analysis. More than 36,000 individual sequences from the region were compared by BLAST[20] with sequences from publicly available databases and were analysed using GRAIL[21] to identify potential coding sequences. In addition, sequences from overlapping BACs were assembled using PHRAP[22–24] and the resulting contigs were also analysed using BLAST and GRAIL to aid in gene prediction. These data were displayed in ACEdb (data available from ncbi.nlm.nih.gov) to visualize predicted exons and their relationships to each other.

Northern blot analysis. Poly(A)$^+$ RNA was extracted from the tissues indicated from wild-type, C3H/HeJ, C3HeB/FeJ-*mg*^{3J}, LDJ/Le-*mg* and C3H/HeJ-*mg*^{L} mice, according to the manufacturer's instructions. RNA STAT-60 (Tel-Test Inc., Friendswood, Texas) was used to isolate total RNA. Poly(A)$^+$ RNA was isolated using the Poly(A)Pure^{TM} messenger RNA purification kit (Ambion Inc., Austin, Texas). 2 μg of each mRNA was separated on a 1% agarose–formaldehyde gel, transferred to nylon and hybridized with a probe for *mg* corresponding to nucleotides 990–1,406 of the murine cDNA sequence, using Rapid-hyb Buffer (Amersham). Filters were washed with 0.1 × SSC (1.5 mM trisodium citrate, 15 mM sodium chloride, pH 7.0), 0.1% SDS and exposed to Kodak X-omat film overnight.

***In situ* hybridization analysis.** Complementary RNA sense and antisense ^{35}S-radiolabelled (10^7 c.p.m.) probes corresponding to nucleotides 677–4,079 of the murine *mg* cDNA sequence were hybridized to 10-μm brain whole-mount coronal sections of C3H/HeJ, LDJ/Le-*mg* and C3HeB/FeJ-*mg*^{3J} animals[25]. Localization of mRNA transcripts was detected by dipping slides in Kodak NBT-2 photoemulsion and exposing for 16 days at 4 °C, followed by development with Kodak Dektol developer. Slides were counterstained with haematoxylin and eosin and photographed. Controls for the *in situ* hybridization experiments included the use of a sense probe, which showed no signal above background levels.

Received 7 October 1998; accepted 8 January 1999.

1. Lane, P. W. & Green, M. C. *Mahogany*, a recessive color mutation in linkage group V of the mouse. *J. Hered.* **51,** 228–230 (1960).
2. Miller, K. A. *et al* Genetic studies of the mouse mutations *mahogany* and *mahoganoid*. *Genetics* **146,** 1407–1415 (1997).
3. Dinulescu, D. M. *et al. Mahogany* (*mg*) stimulates feeding and increases basal metabolic rate independent of its suppression of *agouti*. *Proc. Natl Acad. Sci. USA* **95,** 12707–12712 (1998).
4. Huszar, D. H. *et al.* Targeted disruption of the melanocortin-4 receptor results in obesity in mice. *Cell* **88,** 131–141 (1997).
5. Lu, D *et al.* Agouti protein is an antagonist of the melanocyte-stimulating hormone receptor. *Nature* **371,** 799–802 (1994).
6. Yang, Y. K. *et al* Effects of recombinant agouti-signaling protein on melanocortin action. *Mol. Endocrinol.* **11,** 274–280 (1997).
7. Robbins, L. S. *et al.* Pigmentation phenotypes of variant extension locus alleles result from point mutations that alter MSH receptor function. *Cell* **72,** 827–834 (1993).
8. Mountjoy, K. G., Mortrud, M. T., Low, M. J., Simerly, R.B. & Cone, R. D. Localization of the melanocortin-4 receptor (MC4-R) in neuroendocrine and autonomic control circuits in the brain. *Mol. Endocrinol.* **8,** 1298–1308 (1994).
9. Schultz, J., Milpetz, F., Bork, P & Ponting, C. P. SMART, a simple modular architecture research tool: identification of signaling domains. *Proc. Natl Acad. Sci. USA* **95,** 5857–5864 (1998).
10. Nakayama, M. *et al.* Identification of high-molecular-weight proteins with multiple EGF-motifs by motif-trap screening. *Genomics* **51,** 27–34 (1998).
11. Bork, P. & Beckmann, G. The CUB domain. A widespread module in developmentally regulated proteins. *Mol. Biol.* **231,** 539–545 (1993).
12. Maestrini, E. *et al.* A family of transmembrane proteins with homology to the MET-hepatocyte growth factor receptor. *Proc. Natl Acad. Sci. USA* **93,** 674–678 (1996).
13. Drickamer, K. Multiplicity of lectin-carbohydrate interactions. *Nature Struct. Biol.* **6,** 437–439 (1995).
14. Weis, W. I. & Drickamer, K. Structural basis of lectin-carbohydrate recognition. *Annu. Rev. Biochem.* **65,** 441–473 (1996).
15. Bork, P. & Doolittle, R. F. *Drosophila kelch* motif is derived from a common enzyme fold. *J. Mol. Biol.* **236,** 1277–1282 (1994).
16. Sclessinger, J., Lax, I. & Lemmon, M. Regulation of growth factor activation by proteoglycans: what is the role of low affinity receptors. *Cell* **88,** 357–360 (1995).
17. Shutter, J. R. *et al.* Hypothalamic expression of ART, a novel gene related to *agouti*, is up-regulated in *obese* and *diabetic* mutant mice. *Genes Dev.* **11,** 593–602 (1997).
18. Ollman, M. M. *et al.* Antagonism of central melanocortin receptors *in vitro* and *in vivo* by agouti-related protein. *Science* **278,** 135–138 (1997).
19. Deitrich, W. F., *et al* A comprehensive genetic map of the mouse genome. *Nature* **380,** 149-152 (1996).
20. Altschul, S. F., Gish, W., Miller, W., Myers, E. W. & Lipman, D. J. Basic local alignment search tool. *J. Mol. Biol.* **215,** 403–410 (1990).
21. Uberbacher, F. C. & Mural, R. J. Locating protein-coding regions in human DNA sequences by multiple neural network approach. *Proc. Natl Acad. Sci. USA* **88,** 11261–11265 (1991).
22. Sing, C. F., Haviland, M. B., Wendl, M. C. & Green, P. Base calling of automated sequencer traces using phred. I. Accuracy assessment. *Genome Res.* **8,** 175–185 (1998).
23. Ewing, B. & Green, P. Base calling of automated sequencer traces using phred. II. Error probabilities. *Genome Res.* **8,** 186–194 (1998).
24. Gordon, D., Abajian, C. & Green, P. Consed: a graphical tool for sequence finishing. *Genome Res.* **8,** 195–202 (1998).
25. Duncan, L. *et al.* Down-regulation of the novel gene *Melastatin* correlates with potential for melanoma metastasis. *Cancer Res.* **58,** 1515–1520 (1998).
26. Misumi, D.J. *et al.* The physical and genetic map surrounding the *Lyst* gene on mouse chromosome 13. *Genomics* **40,** 147–150 (1997).
27. Gyapay, G. *et al.* A radiation hybrid map of the human genome. *Hum. Mol. Genet.* **3,** 339–346 (1996).
28. Stewart, E. A. *et al.* An STS-based radiation hybrid map of the human genome. *Genome Res.* **7,** 422–433 (1997).
29. Thompson, J. D., Higgins, D. G. & Gibson, T. J. CLUSTAL W: improving the sensitivity of progressive multiple sequence alignment through sequence weighting, positions-specific gap penalties and weight matrix choice. *Nucleic Acids Res.* **22,** 4673–4680 (1994).
30. Duke-Cohan, J. S. *et al.* Attractin (DPPT-L), a member of the CUB family of cell adhesion and guidance proteins, is secreted by activated human T lymphocytes and modulates immune cell interactions. *Proc. Natl Acad. Sci. USA* **95,** 11336–11341 (1998).

Acknowledgements. We thank I. Jackson for the gift of the C3H/He-*mgL*/*mgL* mice; J. Smutko for mapping the human *mg* orthologue; and M. Donovan, B. Tepper and L. Tartaglia for helpful advice. This work was supported by Hoffman-La Roche Inc.

Correspondence and requests for materials should be addressed to K.J.M. (e-mail: moore@mpi.com). The *mg* cDNA sequence has been deposited at GenBank under accession number AF116897.

The mouse *mahogany* locus encodes a transmembrane form of human attractin

Teresa M. Gunn*, Kimberly A. Miller*, Lin He*, Richard W. Hyman†, Ronald W. Davis†, Arezou Azarani*, Stuart F. Schlossman‡, Jonathan S. Duke-Cohan‡ & Gregory S. Barsh*

** Departments of Pediatrics and Genetics, and the Howard Hughes Medical Institute, and † Department of Biochemistry and the Stanford DNA Sequencing and Technology Center, Stanford University School of Medicine, Stanford, California 94305-5428, USA*

‡ Division of Tumor Immunology, Dana-Farber Cancer Institute, Harvard Medical School, Boston, Massachusetts 02115, USA

Agouti protein and agouti-related protein are homologous paracrine signalling molecules that normally regulate hair colour and body weight, respectively, by antagonizing signalling through melanocortin receptors[1–7]. Expression of *Agouti* is normally limited to the skin, but rare alleles from which *Agouti* is expressed ubiquitously, such as *lethal yellow*, have pleiotropic effects that include a yellow coat, obesity, increased linear growth, and immune defects[8–11]. The *mahogany* (*mg*) mutation suppresses the effects of *lethal yellow* on pigmentation and body weight, and results of our previous genetic studies place *mg* downstream of transcription of *Agouti* but upstream of melanocortin receptors[12]. Here we use positional cloning to identify a candidate gene for *mahogany*, *Mgca*. The predicted protein encoded by *Mgca* is a 1,428-amino-acid, single-transmembrane-domain protein that is expressed in many tissues, including pigment cells and the hypothalamus. The extracellular domain of the *Mgca* protein is the orthologue of human attractin, a circulating molecule produced by activated T cells that has been implicated in